Polymorphism of F-Actin Assembly. 1. A Quantitative Phase Diagram of F-Actin†

Atsushi Suzuki,‡ Masahito Yamazaki,§ and Tadanao Ito*

Department of Biophysics, Kyoto University School of Science, Kyoto 606-01, Japan

Received November 10, 1995; Revised Manuscript Received January 24, 1996⊗

ABSTRACT: We have made the first quantitative phase diagram of actin filament (F-actin) assembly represented by the concentration of F-actin and the χ parameter which characterizes solvent−solute interaction energy. We manipulated the χ value of F-actin by adding a high molecular weight poly(ethylene glycol) with average molecular weight 6000 (PEG 6K). The preferential exclusion of PEG 6K from the region adjacent to F-actin increases the χ value of F-actin. We quantified the PEG 6K-induced increase of the χ value through analysis of the PEG-induced solubility change of protein. The phase diagram shows that F-actin changes its assembly structure from isotropic disordered distribution to anisotropic ordered phase of a lyotropic liquid crystalline with an increase in the concentration and to concentrated anisotropic ordered phase of a crystalline-like bundle with a small increase in χ, respectively, in the physiological concentration range. The formation of the crystalline-like bundle suggests that some specific force may act between F-actin. The present results demonstrate that F-actin can take various assembly structures as observed in cytoplasm by itself, indicating that the versatility of F-actin assembly in cytoplasm may be based on the thermodynamic properties of F-actin as a rod-like molecule.

Actin filament (F-actin) takes various assembly structures in nonmuscle cells, such as a crystalline-like bundle structure in microvilli, a liquid crystalline-like structure in stress fiber and an isotropic gel-like structure in cortex. These individual structures are brought about *in vitro* by actin binding proteins which interact specifically with F-actin (Stossel et al., 1985; Hartwig & Kwiatkowski, 1991). F-Actin is expected to behave as a rod-like molecule in solution. According to the equilibrium properties of rod-like molecules, F-actin may, by itself, take assembly structures similar to those observed in cytoplasm (Flory, 1956). It indicates that the versatility of F-actin assembly in cytoplasm may be based on such thermodynamic properties of F-actin.

Flory (1956) described thermodynamic properties of the rod-like molecule by the χ parameter which characterizes the interaction energy between the solute and solvent. In short, χ represents the free energy change on transferring a solute polymer from the pure to the infinite dilution. The assembly structure has the following characteristic properties. (1) When χ is a negative or a low positive value, a rod-like macromolecule takes isotropic disordered distribution at a low concentration. An increase in the concentration separates the solution into two phases, one is the isotropic distribution phase and the other is a dilute ordered anisotropic phase of lyotropic liquid crystalline. The two phases coexist in a narrow concentration range, and then all molecules take the liquid-crystalline structure. (2) When χ exceeds a critical value, the solution separates into another two phases, the isotropic disordered distribution phase and a concentrated highly ordered anisotropic phase, where the anisotropic phase is predominant. Using poly(benzyl L-glutamate) which takes α-helix conformation in organic solvents, Nakajima et al. (1968) experimentally demonstrated such characteristic properties of a rod-like molecule as predicted by Flory. However, it has been impossible to do such study on biological macromolecules, because of difficulty in changing the χ value systematically in aqueous solution.

Previously, we found that addition of high molecular weight poly(ethylene glycol) (PEG) to actin filament solution changes the assembly structure from isotropic distribution to a crystalline-like bundle structure above a critical concentration of PEG, followed by a rapid increase in the light scattering of the solution. The critical concentration strongly depends on the molecular weight of PEG, and it decreases with an increase in the molecular weight. The effects of PEG were reversible; i.e., the crystalline-like assembly reverted to the isotropic distribution by diluting PEG below the critical concentration, and ovalbumin showed the same effects on the F-actin assembly as PEG (Suzuki et al., 1989). By analyzing the mechanism, we showed that the effects of PEG on F-actin assembly are not due to the direct interaction of PEG with F-actin but due to the indirect interaction that the PEG is preferentially excluded from the region adjacent to F-actin. In that report, we discussed the possibility that the preferential exclusion of PEG increases the χ value in F-actin solution, and the increase of the χ value induces the change of F-actin assembly from the isotropic distribution to the crystalline-like bundle assembly (Suzuki et al., 1989).

In the present report, we have analyzed the effects of such preferential exclusion of PEG by thermodynamics and have succeeded in getting a quantitative relation between the concentration of PEG and the χ value in F-actin solution. This has enabled us to systematically manipulate the χ value in aqueous solution by PEG. Here we report the first quantitative phase diagram of F-actin assembly.

† This work was supported in part by Ministry of Education, Science, Sports and Culture Grant 07808074 to T.I.

* Correspondence should be sent to this author. Tel: 81-75-753-4215. Fax: 81-75-791-0271. E-mail: i54167@sakura.kudpc.kyoto-u.ac.jp.

‡ Present address: Department of Molecular Biology, Yokohama City University School of Medicine, Yokohama 236, Japan.

§ Present address: Department of Physics, Faculty of Science, Shizuoka University, Shizuoka 422, Japan.

⊗ Abstract published in *Advance ACS Abstracts,* April 1, 1996.

0006-2960/96/0435-5238$12.00/0

MATERIALS AND METHODS

General. We used poly(ethylene glycol) with average molecular weight 6000 (PEG 6K) from nakarai tesque (Kyoto, Japan) without further purification except the osmolarity measurement. We purified monomer actin (G-actin) from skeletal muscle by the method of Spudich and Watt (1971). In one preparation, we further purified it by gel filtration chromatography on a Sephacryl S200 column. We could not detect any significant differences between the two preparation methods in our experiments. We polymerized G-actin into filamentous form (F-actin) in F-buffer (100 mM KCl, 2 mM $MgCl_2$, 0.2 mM $CaCl_2$, 0.2 mM ATP, 10 mM imidazole hydrochloride, pH 7.5). We determined the concentration of G-actin from the absorbance of 280 nm wavelength, using the extinction coefficient of 2.66×10^4 M^{-1} cm^{-1}. We measured the 90° light scattering of F-actin solution by using the incident light of 450 nm wavelength.

Measurement of Protein Solubility. We measured solubilities of lysozyme, α-chymotrypsin, ovalbumin, and bovine serum albumin from Sigma Chemical Co. in the presence of PEG 6K by the method of Atha and Ingham (1981). We measured the osmolarity of PEG 6K at room temperature by a thermocouple psychrometer (WESCOR model 5100A). In these experiments, we used PEG 6K purified by recrystallization by the method of Honda et al. (1981).

Determination of Fraction of F-Actin in PEG 6K-Induced Bundle Assembly. We quantified the fraction of F-actin in the PEG-induced bundle assembly by the low centrifugation method as follows. After polymerizing G-actin for 2 h at room temperature in the presence of various concentrations of PEG 6K, we centrifuged the solution at 15000*g* for 30 min. Before the centrifugation, we gently agitated the solution with a couple of upside down inversions to facilitate the equilibrium distribution of F-actin. We estimated the fraction of F-actin in the pellet by measuring the concentration of F-actin in the supernatant by the Bio-Rad dye-based assay.

Electron Microscopy. We adsorbed the sample solution on a carbon-coated collodion grid for 1 min, washed it with the same buffer as the solution, and then negatively stained the sample with 4% uranyl acetate for 1 min. To avoid shear force which may affect the sample structure, we carried out the manipulation by putting the grid on a drop of each solution without removing the remaining solution by filter paper. We observed the image of the sample by a JOEL 100 B electron microscope under 80 kV of accelerating voltage.

RESULTS

PEG 6K-Induced Bundle Formation. Addition of PEG 6K to a dilute F-actin solution brings about an abrupt transition of the assembly structure of F-actin from an isotropic disordered distribution to a concentrated highly ordered bundle of a crystalline-like structure above a critical concentration of PEG 6K (Figure 1A; Suzuki et al. 1989). The formation of the bundle is accompanied by an abrupt increase in the light scattering of the F-actin solution (open circles in the inset of Figure 1B). The light scattering reaches a plateau value very gradually when the F-actin solution stands without any agitation (>10 h). On the other hand, the light scattering reaches the same plateau value shortly after a mild agitation of the solution with a couple of upside down inversions (open circles in Figure 1B). At a concentration of PEG 6K just below the critical concentration at which the bundle formation begins, the increase in the light scattering does not occur even when the solution is subjected to the upside down inversions (closed circles in Figure 1B). These results show that the PEG-induced bundle formation is diffusion limited, and the shear alignment by the upside down inversion should facilitate to take the equilibrium distribution (see Discussion for details). As analyzed in Suzuki et al. (1989), this change in the assembly structure of F-actin is attributed to a phase transition of F-actin assembly from the homogeneous phase of the isotropic disordered distribution to the heterogeneous phase of the

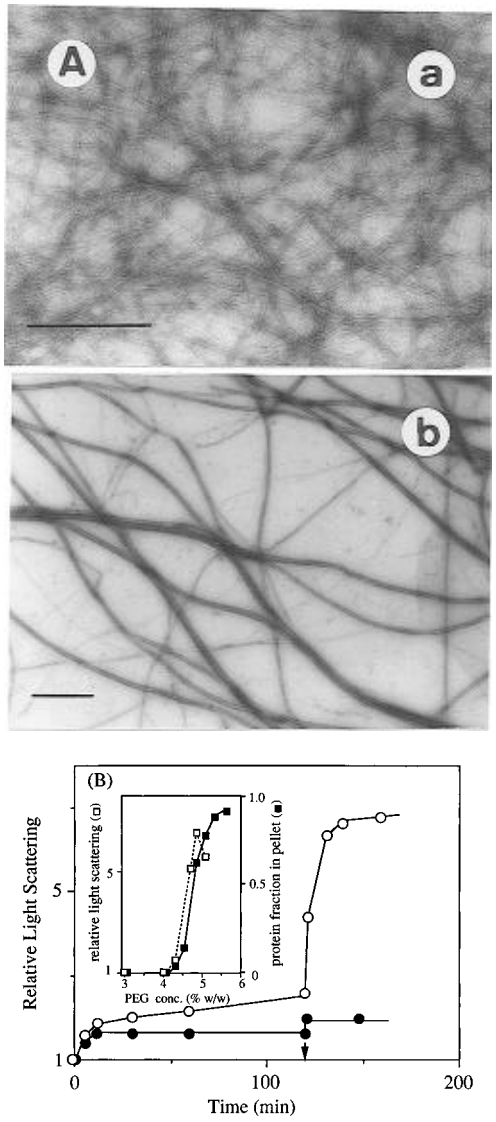

FIGURE 1: Electron microscopic morphology of F-actin assembly (A) and light scattering in F-actin solution (B) below and above the critical concentration of PEG 6K. In (A), G-actin (0.5 mg/mL) was polymerized in F-buffer containing 4.0% or 4.5% PEG 6K for 2 h at room temperature and then mildly pipetted before being adsorbed to the grid for electron microscopy. Each sample was negatively stained with 4% uranyl acetate as described under Materials and Methods. The photographs show F-actin prepared at 4.0% (a) and at 4.5% (b) PEG 6K, respectively. Bar, 0.5 μm. In (B), G-actin (0.5 mg/mL) was added to F-buffer containing 4.0% (●) or 4.5% (○) PEG 6K in an optical cuvette, and the time course of a change in the light scattering was measured. At the time indicated by the arrow, the solution was gently agitated with a couple of upside down inversions. In the inset of (B), the intensity of the light scattering (□) and the fraction of F-actin precipitated by centrifugation at 15000*g* for 30 min (■) after the upside down inversions are plotted against the concentrations of PEG 6K.

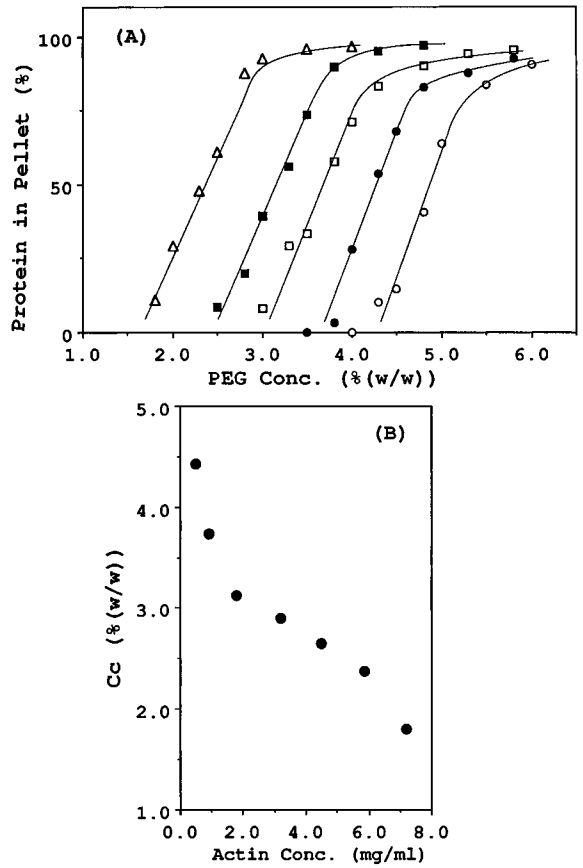

FIGURE 2: Dependence of the precipitate phase formation on F-actin concentration. F-Actin of an appropriate concentration was prepared in the presence of various concentrations of PEG 6K. The fraction of F-actin in the PEG-induced bundle assembly (precipitate phase) was quantified by the low-speed centrifugation method as described under Materials and Methods. In (A), the percentage of F-actin in the precipitate phase is plotted against the concentration of PEG 6K. The concentrations of F-actin are 7.2 mg/mL (△), 4.5 mg/mL (■), 1.8 mg/mL (□), 0.9 mg/mL (●), and 0.5 mg/mL (○), respectively. In (B), the critical concentration of PEG 6K to induce the precipitate phase is plotted against F-actin concentration. The critical concentration was determined from the concentration of PEG 6K required to precipitate 10% of total F-actin.

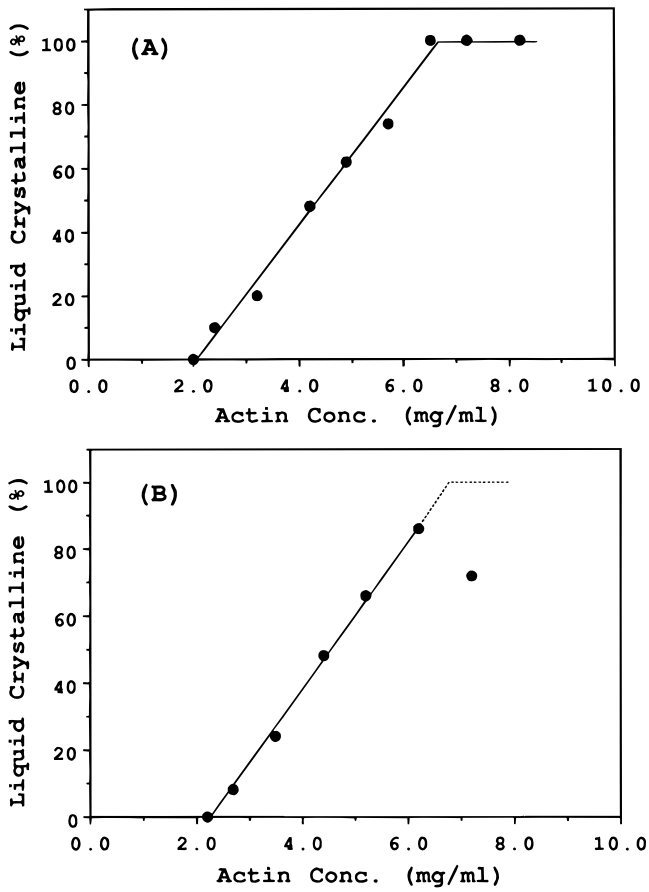

FIGURE 3: Effect of PEG 6K on liquid-crystalline formation. F-Actin of various concentrations was prepared in the presence of 2% PEG 6K or in its absence. The fraction of F-actin of the liquid-crystalline phase was quantified from birefringence of the solution by the method of Suzuki et al. (1991) and plotted against F-actin concentration. (A) Liquid-crystalline formation in the absence of PEG 6K. (B) Liquid-crystalline formation in the presence of 2% PEG 6K.

isotropic disorder distribution and the concentrated highly ordered assembly.

In the present report, we quantified the fraction of F-actin in the PEG 6K-induced bundle assembly as follows. After polymerizing G-actin completely in the presence of various concentrations of PEG 6K, we gently agitated the solution with a couple of upside down inversions to facilitate the equilibrium distribution and then centrifuged it at 15000*g* for 30 min. We estimated the fraction of F-actin in the pellet by measuring the concentration of F-actin in the supernatant. The centrifugation could selectively precipitate F-actin in the bundle assembly but not at all F-actin in the isotropic disordered distribution (see inset of Figure 1B). Hence, we call the bundle assembly the precipitate phase hereafter.

Concentration of PEG 6K on the Boundary of Homogeneous and Heterogeneous Phases. To determine the concentration of PEG 6K on the boundary of the homogeneous phase of the isotropic distribution and the heterogeneous phase of the coexistence of the isotropic distribution and the bundle assembly, we measured the fraction of the precipitate phase at various concentrations of PEG 6K (Figure 2). We defined the concentration of the PEG to precipitate 10% of F-actin as the concentration, C_c, in the phase boundary. Figure 2B shows C_c values at various concentrations of F-actin. C_c values decreased with an increase in F-actin concentration. It should be noted that the slope of C_c change becomes rather gentle in F-actin concentrations larger than 2 mg/mL.

Effect of PEG 6K on Liquid-Crystalline Formation. In our previous paper (Suzuki et al., 1991), we reported that F-actin forms a dilute anisotropic phase of a lyotropic liquid-crystalline structure with an increase in the concentration of F-actin. We call this phase the liquid-crystalline phase. F-actin in the liquid-crystalline phase is highly ordered and shows optical birefringence. As reported in the above paper, we succeeded in quantifying the fraction of the liquid-crystalline phase by measuring optical birefringence. On the basis of this work, we have investigated effects of PEG 6K on the formation of the liquid-crystalline phase (Figure 3). The liquid-crystalline phase appears at 2 mg/mL F-actin in the absence of PEG (Figure 3A). The fraction of the liquid-crystalline phase increased linearly with an increase in the concentration, and all F-actin took the liquid-crystalline phase above 6.5 mg/mL. The presence of 2% PEG 6K did not significantly affect the formation of the liquid-crystalline phase (Figure 3B), although the observed value at 7.2 mg/mL deviated from the expected one. The deviation may be due to the formation of a small amount of the precipitate phase at the concentration of PEG (see Figure 2).

Phase Diagram of F-Actin Assembly. Flory (1956) represented the phase diagram of the assembly structure of

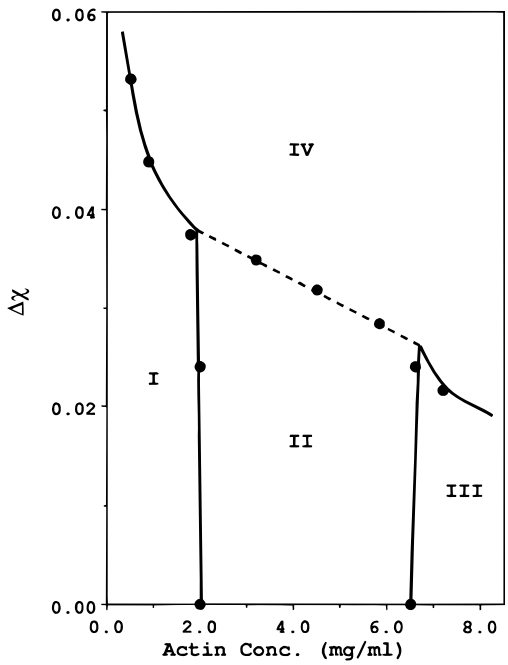

FIGURE 4: Phase diagram of F-actin assembly. The phase boundary was determined from the results shown in Figures 2 and 3. The $\Delta\chi$ value in the vertical line was determined from the concentration of PEG 6K by eq 1. The regions denoted as I−IV in the figure represent the regions of the isotropic disordered phase (I), coexistence of isotropic disordered phase and dilute anisotropic phase of lyotropic liquid crystalline (II), lyotropic liquid-crystalline phase (III), and coexistence of isotropic disordered phase and concentrated anisotropic ordered phase (precipitate phase) (IV), respectively.

rod-like solute polymer by a thermodynamic parameter, χ: χ is defined as the free energy change per segment divided by the product of the universal gas constant (R) and the thermodynamic temperature (T) on transferring a solute polymer from the pure to the infinite dilution, where the segment is defined as the axial ratio of the polymer (length to diameter).

In our previous work (Suzuki et al., 1989), we showed that the effect of PEG on F-actin assembly is due to an indirect interaction of PEG with F-actin. The χ value is increased by the preferential exclusion of PEG from the region adjacent to F-actin. In the present paper, we have succeeded in quantifying the effect of such preferential exclusion of PEG 6K on the χ value in F-actin solution (see Appendix). By taking a subunit actin of F-actin as the segment, we obtained a quantitative relation between the concentration of PEG 6K and the χ value:

$$\Delta\chi = (1.2 \times 10^{-2})C \qquad (1)$$

where $\Delta\chi$ represents the increase in the χ value caused by the addition of C% (w/w) of PEG 6K. $\Delta\chi$ in eq 1 is not the absolute χ value but the difference between those values in the presence (χ) and in the absence (χ_0) of PEG 6K; i.e., $\Delta\chi = \chi - \chi_0$. χ_0 represents the χ value in F-buffer (100 mM KCl, 2 mM $MgCl_2$, 0.2 mM $CaCl_2$, 0.2 mM ATP, 10 mM imidazole hydrochloride, pH 7.5). In this report, we discuss the phase diagram of F-actin by using the concentration of F-actin (mg/mL) and the $\Delta\chi$ value (Figure 4).

The phase diagram shows that F-actin of a dilute concentration takes the isotropic disordered phase under a low $\Delta\chi$ value (a in Figure 1A, I in Figure 4). As the concentration exceeds 2 mg/mL, the solution separates into two phases, one is the isotropic disordered phase and the other the liquid-crystalline phase (II in Figure 4). As previously analyzed by us, the liquid-crystalline phase is highly ordered, in which the long axis of F-actin is distributed within ∼15° (Suzuki et al., 1991). In this coexistence region, the concentrations of F-actin in both the isotropic and the liquid-crystalline phases are constant, 2 and 6.5 mg/mL, respectively. At a concentration beyond 6.5 mg/mL (III in Figure 4), all F-actin takes the liquid-crystalline phase, where the distribution becomes more ordered, e.g., ∼7° at 7.7 mg/mL (Suzuki et al., 1991).

Of great interest is a sudden appearance of the precipitate phase with a small increase in $\Delta\chi$ (IV in Figure 4). F-actin (0.5 mg/mL) takes the isotropic disordered phase at $\Delta\chi$ = ∼0.05 (a in Figure 1A). When the $\Delta\chi$ value increases only by 0.006, the precipitate phase becomes dominant, where F-actin takes a concentrated highly ordered anisotropic assembly of a crystalline-like structure (b in Figure 1A). The increase in $\Delta\chi$ means the decrease in the affinity of F-actin with the solvent, and the value corresponds to 0.006RT/mol of subunit.

The critical $\Delta\chi$ value to induce the precipitate phase decreases with an increase in the concentration of F-actin (Figure 4). The value decreases more rapidly in the isotropic phase (I in Figure 4) than in the heterogeneous phase where the isotropic and the liquid-crystalline phases coexist (II in Figure 4). In the heterogeneous phase, the critical $\Delta\chi$ value decreases linearly with an increase in the concentration of F-actin (dotted line in Figure 4).

DISCUSSION

Manipulation of the χ Value by PEG. The method to manipulate the χ value in F-actin solution applied here is based on a well-analyzed phenomenon that a high molecular weight inert molecule in protein solution is preferentially excluded from the region adjacent to the protein surface (Kuntz & Kauzmann, 1974; Arakawa & Timasheff, 1985a,b). To quantify the effect on the χ value by thermodynamics, no significant assumption has been required, as shown in the Appendix. The most important advantage of this method is to be able to systematically manipulate the χ value without changing the pH and ionic condition which are essential in keeping biological molecules intact.

Equilibrium Distribution of F-Actin. The PEG-induced bundle formation proceeds very slowly when the F-actin solution stands without any agitation. It takes more than 10 h to reach an equilibrium value. On the other hand, the formation reaches the same equilibrium value shortly after a mild agitation of the solution with a couple of upside-down inversions (Figure 1B). The liquid-crystalline formation by an increase in the concentration of F-actin proceeds in a similar way, and it is also accelerated by the upside down inversions (Suzuki et al., 1991). These results should be interpreted in terms of the mobility of F-actin in the solution.

Recently, Käs et al. (1996) extensively studied the mobility of single actin filaments in F-actin solutions ranging from 0.2 to 4.0 mg/mL, using fluorescence video microscopy to visualize single fluorescence-labeled actin filaments. The single actin filaments are mobile along the virtual tube formed around a filament in a matrix of unlabeled F-actin. The self-diffusion coefficient along the tube ranges from 7 $\times 10^{-14}$ to 5 $\times 10^{-15}$ m^2/s. In addition, alignment of actin filaments begins to occur shortly after the actin filaments

are subjected to shear stress and the filaments relax into the original distribution after 2−3 h. Such mobility of actin filaments may well explain the above-described results of the PEG-induced bundle and the liquid crystalline formations. The rate-determining step of these formations is the alignment of F-actin. The self-diffusion of single actin filaments may cause spontaneous alignment of F-actin originally distributed isotropically, but such alignment should proceed very slowly owing to the difficulty in changing the filament orientation by the slow anisotropic diffusion as described above, so that F-actin requires such a long time to reach the new equilibrium distribution. On the other hand, the upside down inversions enable F-actin to rapidly reach the same equilibrium distribution through the shear alignment of the filaments, as shown in Figure 1B. This shear alignment-accelerated redistribution of F-actin should be the true equilibrium distribution, because such redistribution does not occur below the critical concentration, i.e., 4.5% (w/w) PEG 6K for the bundle formation at 0.5 mg/mL F-actin (Figure 1B) or 2 mg/mL F-actin for the liquid-crystalline formation (Figure 3).

Phase Diagram of F-Actin. The phase diagram presented here is the first quantitative phase diagram of F-actin whose assembly structures play important roles in biological functions. There have been several reports about the change in the assembly structures caused by nonphysiological conditions such as low pH and high divalent cations, but no systematic analysis has been done until now (Kawamura & Maruyama, 1970; Hanson, 1973).

The phase diagram shows that F-actin behaves as a rod-like molecule thermodynamically, and it takes various assembly structures similar to those observed in cells at the physiological concentrations as a direct consequence of its thermodynamic properties. At concentrations below 2 mg/mL, F-actin takes isotropic disorder distribution (isotropic disordered phase), and with an increase in the concentration and in χ, the assembly is transformed into a dilute anisotropic ordered assembly of a lyotropic liquid-crystalline (liquid crystalline phase) and into a concentrated anisotropic ordered assembly of a crystalline-like bundle (precipitate phase), respectively (Figure 4).

The result that the formation of the liquid-crystalline phase is independent of the $\Delta\chi$ value indicates that an attractive interaction between F-actin does not affect the liquid-crystalline formation. Hence, the formation is considered to be purely entropic, as predicted theoretically for a rod-like molecule (Onsager, 1949; Ishihara, 1951; Flory, 1956). That is, the number of random configurations of F-actin as a "rod" in limited space decreases drastically with an increase in the concentration so that some fraction of F-actin changes the configuration into the anisotropic ordered array above a critical concentration. As shown in our previous work (Suzuki et al., 1991), the critical concentration increases with a decrease in its length with the relation that $V_c = 2.5/x$, where V_c is the volume fraction of F-actin with the axial ratio (length to diameter) of x. The value coincides well with 3.4 obtained by Onsager (1949) or Ishihara (1951) from consideration of the second virial coefficient, though it is somehow smaller than 8.0 obtained by Flory (1956) from his lattice model.

It is surprising, though expected theoretically, that a small increase in the $\Delta\chi$ value by 0.006 drastically changes the assembly structure of F-actin from the isotropic disordered distribution to the anisotropic ordered array of a crystalline-like bundle (Figures 1 and 4). This increase in the $\Delta\chi$ value corresponds to a decrease in the affinity of F-actin with the solvent. It is $\sim$0.006RT/mol for subunit actin and $\sim$10RT/mol for F-actin with 5 μm length. The value may be negligibly small for subunit actin but significantly large for F-actin to change its assembly structure. The above phase behavior of F-actin solution may be explained qualitatively by the theoretical analysis for the equilibrium properties of a rod-like molecule (Flory, 1956). The mixing entropy for F-actin as a rod at equilibrium disorder is much lower than that of a globular protein. Hence, a small change in χ suddenly "precipitates" F-actin.

The critical value of $\Delta\chi$ to induce the precipitate phase rapidly decreases with an increase in the concentration of F-actin in the isotropic disordered phase (I in Figure 4). This should be attributed to a rapid decrease in entropy of the random configuration with an increase in the concentration, as discussed above. In the heterogeneous phase (II in Figure 4), the $\Delta\chi$ value decreases linearly with an increase in the concentration (dotted line in Figure 4). According to the phase rule, the increase in F-actin concentration varies the fraction of F-actin taking either isotropic disordered assembly or liquid-crystalline assembly without affecting entropy of the individual assembly structures in this region. In this case, the critical value, $\Delta\chi$, can be represented as $\Delta\chi = f_l\Delta\chi_l + (1 - f_l)\Delta\chi_i$, where f_l is the molar fraction of F-actin taking the liquid crystalline assembly. $\Delta\chi_l$ and $\Delta\chi_i$ are the critical values of the liquid-crystalline phase and the isotropic disordered phase at the boundaries of the coexistence phase, which are evaluated as 0.038 and 0.027, respectively. As f_l increases in proportion to an increase in F-actin concentration, the $\Delta\chi$ value decreases linearly with the increase in the concentration as shown by the dotted line in Figure 4. The difference between $\Delta\chi_l$ and $\Delta\chi_i$ may be attributed mainly to the difference in the assembly structure of F-actin in the individual phases. In the liquid-crystalline phase where F-actin is highly ordered, a comparatively small χ may precipitate F-actin as a direct consequence of a smaller change in the entropy.

The observed crystalline-like structure of F-actin in the precipitate phase could not be expected to be produced only by a nonspecific force such as χ (b in Figure 1A). Some specific interaction force which is operable only for more highly ordered arrangement should be required for the existence of the crystalline-like structure. A small supplementation of such a specific force would be sufficient to bring about it, since little further sacrifice of entropy is required in transformation to crystalline regularity in the precipitate phase. It is interesting that F-actin capped at the barbed end by an actin binding protein such as gelsolin cannot take such crystalline-like structure in the precipitate phase (Suzuki & Ito, 1996).

In nonmuscle cell, F-actin takes various assembly structures such as an isotropic disordered structure in cortex, a liquid-crystalline-like bundle in stress fiber, and a crystalline-like ordered structure in microvilli. Each of these structures plays an important role in cell functions (Stossel, 1984, 1994; Bretcher, 1991). From biological viewpoints, it may be of great importance that the phase diagram shows the ability of F-actin to take all of these structures by itself in the physiological concentration range. It indicates that the versatility of F-actin assembly in cytoplasm may be based on the thermodynamic properties of F-actin as a rod as discussed here. In cytoplasm, the concentrated ordered

structure of F-actin should be more preferable than in the buffered solution without protein, for proteins in cytoplasm may have a similar exclusion effect on the χ value as discussed here for PEG. In fact, we observed that F-actin takes the crystalline-like structure in the solution containing 15% (w/w) ovalbumin (Suzuki et al., 1989). These results suggest that F-actin in cytoplasm might exist near the boundary of the phase shown in Figure 4. Hence, F-actin could dynamically change its assembly structure in cytoplasm with a small supplementation of energy.

The individual assembly structures of F-actin observed in cytoplasm are brought about *in vitro* by various kinds of actin binding proteins which specifically interact with actin (Stossel et al., 1985, Hartwig & Kwiatkowski, 1991). The number of actin binding proteins found until now has been more than 50. As shown here, F-actin has the ability to make those assembly structures as a direct consequence of its thermodynamic properties as a rod, and the individual assembly structures have different physicochemical properties which may play important roles in cell functions (Oster, 1984; Ito et al., 1987, 1992; Janmey, 1991). In order to stabilize the individual assembly, or to change them dynamically, this many actin binding proteins might have been selected in various kinds of organisms through the process of evolution.

APPENDIX

Quantification of the Effect of PEG on the χ Value. χ represents the free energy change per unit segment divided by *RT* on transferring a solute polymer from the pure to the infinite dilution, where *R* and *T* are the universal gas constant and the thermodynamic temperature, respectively (Flory, 1956). In the analysis by Flory, a rod-like molecule with the axial ratio (length to diameter) of *x* has *x* pieces of segment. In our analysis for F-actin, we define a subunit actin as unit segment, and so F-actin composed of *n* subunit actins has *n* pieces of segment.

χ depends on the nature of the solvent to which the solute is transferred. The difference in χ ($\Delta\chi$) between different kinds of solvents is related to the difference in the chemical potential of solute ($\Delta\mu_2$) in the individual solvents:

$$\Delta\mu_2 = RT\Delta\chi n(1 - \upsilon_2)^2 \quad (1)$$

where υ_2 and *n* are the volume fraction and the segment number of the solute polymer, respectively (Flory, 1956). We discuss here the effect of PEG on the χ value theoretically at first, and show the way to quantify it.

Theory. In a ternary system composed of component 1 (water), component 2 (F-actin), and component 3 (PEG), the following relation can be derived by using the standard cross-differentiation relation at equilibrium (Casassa & Eisenberg, 1964):

$$(\partial\mu_2/\partial m_3)_{T,m_2} = -(\partial m_3/\partial m_2)_{T,\mu_1,\mu_3}(\partial\mu_3/\partial m_3)_{T,m_2} \quad (2)$$

where m_i and μ_i are the molar concentration (mol/mL·H_2O) and the chemical potential of component i, respectively.

It is a well-established concept which is probed experimentally that inert polymer such as high molecular weight PEG in protein solution is preferentially excluded from the region near the protein surface by steric hindrance (Kuntz & Kauzmann, 1974; Arakawa & Timasheff, 1985a,b). For example, the measured value of $(\partial m_3/\partial m_2)_{T,\mu_1,\mu_3}$ in protein solutions containing PEG as cosolvent is negative for PEG with average molecular weight larger than 400, and a larger PEG gives a larger negative value (Arakawa & Timasheff, 1985a). These results directly show that PEG is preferentially excluded from the region adjacent to the protein surface in a molecular weight-dependent manner. To evaluate the effect of such preferential exclusion in eq 2, we introduced an exclusion layer near the surface of component 2, from which component 3 is excluded. Setting the volume of the exclusion layer per mole of component 2 as V_{exc}, we can conduct eq 3:

$$(\partial m_3/\partial m_2)_{T,\mu_1,\mu_3} = -V_{exc}m_3^0 \quad (3)$$

where m_3^0 is the concentration of component 3 in the bulk phase, which should be equal to the concentration in the absence of component 2.

We related $(\partial\mu_3/\partial m_3)_{T,m_2}$ of eq 2 to the osmolarity, C_π, of component 3 as follows. The Gibbs−Duhem equation gives the relation that

$$(\partial\mu_1/\partial m_3)_{T,m_2} + V_1m_2(\partial\mu_2/\partial m_3)_{T,m_2} + V_1m_3(\partial\mu_3/\partial m_3)_{T,m_2} = 0 \quad (4)$$

where V_1 represents the partial molar volume of component 1. From eqs 2−4

$$(\partial\mu_3/\partial m_3)_{T,m_2} = -1/V_1(1/m_3)\{1/[1 + V_{exc}(m_3^0/m_3)m_2]\}(\partial\mu_1/\partial m_3)_{T,m_2}$$

If $V_{exc}m_2 << 1$, $m_3^0/m_3 = 1/(1 - V_{exc}m_2) \approx 1$. Thus

$$(\partial\mu_3/\partial m_3)_{T,m_2} = -1/V_1(1/m_3)(\partial\mu_1/\partial m_3)_{T,m_2} = RT(1/m_3)(\partial C_\pi/\partial m_3)_{T,m_2} \quad (5)$$

where C_π is the osmolarity of component 3. From eqs 2, 3, and 5

$$(\partial\mu_2/\partial m_3)_{T,m_2} = RTV_{exc}(m_3^0/m_3)(\partial C_\pi/\partial m_3)_{T,m_2} = RTV_{exc}(\partial C_\pi/\partial m_3)_{T,m_2}$$

$$\Delta\mu_2 = RTV_{exc}C_\pi \quad (6)$$

In a dilute solution where the volume fraction of the solute polymer, υ_2, is negligible, the following relation is derived from eqs 1 and 6:

$$\Delta\chi = \Delta\mu_2/RTn = V_{exc}C_\pi/n \quad (7)$$

Experiments. The validity of eq 6 was tested in the experiments to measure a change in protein solubility induced by PEG. In the above ternary system, the solubility change of component 2 by the addition of component 3 can be represented as

$$\ln S/S_0 = -\Delta\mu_2/RT = -V_{exc}C_\pi \quad (8)$$

where S_0 and *S* are the solubilities of component 2 in the absence and presence of component 3, respectively (Arakawa & Timasheff, 1985a,b). Equation 8 indicates that the log scale value of solubility of component 2 should be linear against the osmolarity of component 3, with a slope equal to the exclusion volume, V_{exc}.

Figure 5 shows the experimental results of PEG 6K-induced change in protein solubility for lysozyme, α-chymotrypsin, ovalbumin, and bovine serum albumin. As predicted in eq 8, the log scale values of the solubilities of the individual proteins decreased linearly against the osmo-

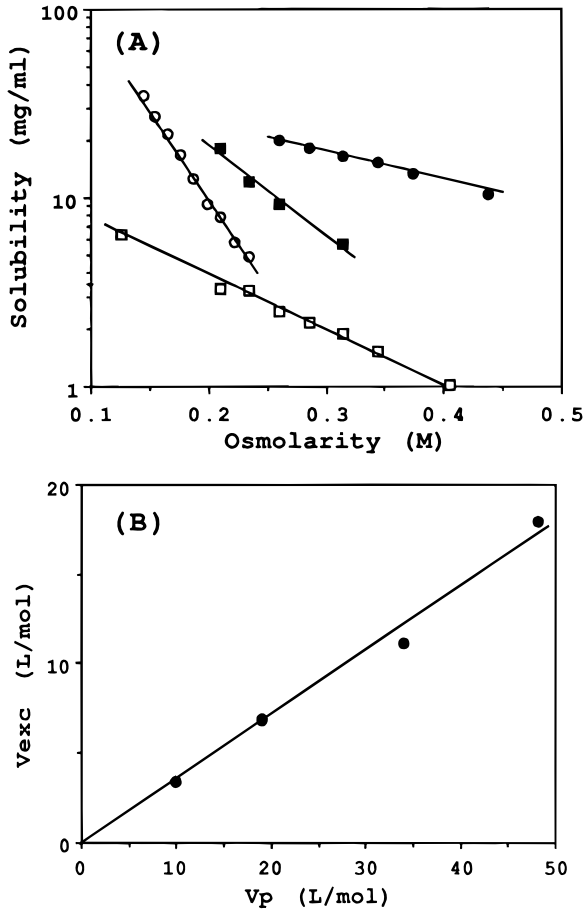

FIGURE 5: Effect of PEG 6K on protein solubility. Solubilities of various kinds of protein were measured in the presence of PEG 6K by the method of Atha and Ingham (1981). In (A), the values of solubility (log scale) are plotted against osmolarities of PEG 6K: (●) lysozyme, (□) chymotrypsin, (■) ovalbumin, and (○) bovine serum albumin. In (B), the exclusion volume (V_{exc}) of each protein obtained from slope of the line in (A) is plotted against partial molar volume of the protein. See Appendix for details.

larity of PEG 6K (Figure 5A). The V_{exc} values estimated from the individual slopes are 3.4, 6.9, 11.1, and 18.0 L/mol for lysozyme, α-chymotrypsin, ovalbumin, and bovine serum albumin, respectively. All of these values satisfy the condition of $m_2V_{exc} << 1$ to derive eq 6 at all the concentrations of the individual proteins used in the experiments. In addition, the V_{exc} value is proportional to the partial molar volume of the protein, V_p, irrespective of difference in chemical properties of the individual proteins (Figure 5B). These results are expected from the theoretical model described above, because the exclusion layer is expected to increase with an increase in the volume of protein. We found the following relation from the results:

$$V_{exc} = 0.36V_p \quad \text{for PEG 6K} \tag{9}$$

Using the relation in eq 9, we estimated the exclusion distance measured from the center of protein, r, within which PEG 6K may not access the protein. Setting the radius of protein as r_0

$$V_{exc}/V_p = [(r/r_0)^3 - 1] = 0.36$$

$$r = 1.1r_0 \tag{10}$$

Evaluation of Exclusion Volume and χ Value for F-Actin. F-Actin is a rod-like molecule which is composed of several hundred subunit actins. As the relation in eq 9 was obtained for globular proteins, we could not evaluate the exclusion volume of F-actin directly from the relation. We estimated the value by assuming that PEG 6K is inaccessible to F-actin within a distance 1.1 times as long as the radius of the cross section, r_0, as indicated in eq 10. The volume of a rod is proportional to the area of the cross section. Thus

$$V_{exc} = [(r/r_0)^2 - 1]V_f = 0.21V_f = 0.21nV_g$$

where V_f is the molar volume of F-actin and V_g and n are the molar volume and the number of subunit actins in the filament, respectively. Taking 34 L/mol as the V_g value, which is equal to the partial molar volume of G-actin, we got $V_{exc} = 7.1n$ (L/mol).

The concentration of PEG used in the experiments of F-actin was less than 5% (w/w). We confirmed that the osmolarity of PEG 6K can be approximated as its molar concentration in this concentration range. Hence, by setting the molar concentration of PEG 6K in place of C_π in eq 7, we evaluated the increase of the χ value, Δχ, of F-actin caused by the addition of C% (w/w) of PEG 6K as

$$\Delta\chi = (1.2 \times 10^{-2})C$$

REFERENCES

Arakawa, T., & Timasheff, S. N. (1985a) *Biochemistry 24*, 6756−6762.

Arakawa, T., & Timasheff, S. N. (1985b) *Methods Enzymol. 114*, 49−77.

Atha, D. H., & Ingham, K. C. (1981) *J. Biol. Chem. 256*, 12108−12117.

Bretcher, A. (1991) *Annu. Rev. Cell Biol. 7*, 337−374.

Casassa, E. F., & Eisenberg, H. (1964) *Adv. Protein Chem. 19*, 287−395.

Flory, P. J. (1956) *Proc. R. Soc. London, A 234*, 73−89.

Hanson J. (1973) *Proc. R. Soc. London, B 183*, 39−58.

Hartwig, J. H., & Kwiatkowski, D. J. (1991) *Curr. Opin. Cell Biol. 3*, 87−97.

Honda, K., Maeda, Y., Sasakawa, S., Ohno, H., & Tsuchida, E. (1981) *Biochem. Biophys. Res. Commun. 101*, 165−171

Ishihara, A. (1951) *J. Chem. Phys. 19*, 1142−1147.

Ito, T., Zaner, K. S., & Stossel, T. P. (1987) *Biophys. J. 51*, 745−753.

Ito, T., Suzuki, A., & Stossel, T. P. (1992) *Biophys. J. 61*, 1301−1306.

Janmey, P. A. (1991) *Curr. Opin. Cell Biol. 3*, 4−11.

Kawamura, K., & Maruyama, K. (1970) *J. Polym. Sci. 44*, 51−69.

Käs, J., Strey, H., Tang, J., Ezzell, R., Sackmann, E., & Janmey, P. A. (1996) *Biophys. J. 70*, 609−625.

Kuntz, I. D., & Kauzmann, W. (1974) *Adv. Protein Chem. 28*, 239−338.

Nakajima, A., Hayashi, T., & Ohmori, M. (1968) *Biopolymers 6*, 973−982.

Onsager, L. (1949) *Ann. Rev. N.Y. Acad. Sci. 51*, 627−659.

Oster, G. (1984) *J. Embryol. Exp. Morphol. 83* (Suppl.), 329−364.

Spudich, J. A., & Watt, S. J. (1971) *J. Biol. Chem. 246*, 4866−4871.

Stossel, T. P. (1984) *J. Cell Biol. 99*, 15s-19s.

Stossel, T. P. (1994) *Sci. Am. 271*, 40−47.

Stossel, T. P., Chaponnier, C., Ezzell, R. M., Hartwig, J. H., Janmey, P. A., Kwiatkowski, D. J., Lind, S. E., Smith, D. B., Southwick, F. S., Yin, H. L., & Zaner, K. S. (1985) *Annu. Rev. Cell Biol. 1*, 353−402.

Suzuki, A., & Ito, T. (1996) *Biochemistry 35*, 5245−5249.

Suzuki, A., Yamazaki, M., & Ito, T. (1989) *Biochemistry 28*, 6513−6518.

Suzuki, A., Maeda T., & Ito, T. (1991) *Biophys. J. 59*, 25−30.

BI952693F